Marine and Petroleum Geology
June 2010, Volume 27, Issue 6, Pages 1157-1165
http://dx.doi.org/10.1016/j.marpetgeo.2010.03.002

Experimental study of gas hydrate formation and destabilisation using a novel high-pressure apparatus

L. Ruffine[a, *], J.P. Donval[a], J.L. Charlou[a], A. Cremière[a] and B.H. Zehnder[b]

[a] IFREMER, Centre de Brest, Département de Géosciences Marines, 29280 Plouzané, France
[b] SITEC-Sieber Engineering AG, Aschbach 621, CH – 8124 Maur, Switzerland

*: Corresponding author : L. Ruffine, Tel.: +33 2 98 22 48 88; fax: +33 2 98 22 45 70, email address : Livio.Ruffine@ifremer.fr

Abstract:

A novel variable-volume type high-pressure apparatus has been designed, constructed and used for gas hydrate investigations. The apparatus has an operating temperature ranging from 253 K to 473 K and pressure ranging from 0.1 MPa to 60 MPa. Its central component consists of a viewing windows cell to which several sensors or analytical instruments can be connected. At its present configuration, a Raman spectrometer and a gas chromatograph are connected for the study of the liquid (or solid) and the gas phases respectively.

The apparatus was used for the study of two different systems. The first system was composed of carbon dioxide (CO2) and water for which the hydrate formation and dissolution has been investigated by injecting water into liquid CO2. The evolution of the system was monitored by means of visual observation in combination with Raman spectroscopy. The second system consists of thermogenic-like gases (i.e. synthetic natural gas) for which the hydrate formation and dissociation have additionally been investigated by monitoring the change of the vapour phase composition. The consequences of the destruction of the hydrate skin formed at the water–gas interface have been studied. Thus, an attempt has been made to study the importance of the interfacial contact layer between the gas phase and the aqueous phase for the hydrate growth process. In this paper, we describe in detail the apparatus, followed by the presentation of the results on both systems investigated.

Keywords : Gas hydrates, thermogenic, carbon dioxide, formation, destabilisation, novel apparatus, Raman spectroscopy, chromatography.

1 Introduction

Natural gas hydrates are generally defined as insertion compounds formed from water and light hydrocarbons, mainly methane (Sloan and Koh, 2007). The whole structure is stabilised by interactions between the water molecules forming a lattice and the gas molecules contained within this lattice. Hydrates have been studied worldwide for many years, mainly because they have been problematic in gas production and transport (Briaud and Chaouch, 1999; Hammerschmidt, 1934). Their formation within pipelines slows down and blocks flow with significant economic impact. At present, natural gas hydrate production is being investigated by the oil and gas industry for its potential as a promising and sustainable energy resource, as its estimated abundance may represents more than twice the combined carbon of coal, conventional gas and petroleum (Collet and Kuuskraa, 1998; Makogon et al., 2007; Max, 2003; Max et al., 2006; Milkov and Sassen, 2002; Moridis, 2003; Moridis et al., 2009; Moridis et al., 2004; Moridis and Sloan, 2007). In addition, gas hydrate reservoirs could be a real option for CO_2 sequestration (House et al., 2006; Kwon et al., 2008; Lee et al., 2002; White, 2008)**.** Therefore, there is great interest in both understanding the formation, accumulation and dissociation or dissolution of gas hydrates and developing economically viable processes for natural-gas hydrate production (Goel, 2006; Lee et al., 2002; Madden et al., 2009; Torres et al., 2008; Walsh et al., 2008). Moreover, hydrate-based technology for separation processes is also under intensive development as shown by the drastic increase in publications issued (Duc et al., 2007; Englezos and Lee, 2005; Li et al., 2009; Linga et al., 2008; Purwanto et al., 2001).

Although a significant amount of research on gas hydrates has been carried out in both industrial and academic laboratories, several study areas such as the formation mechanism and the hydrate growth are still poorly understood, especially for complex systems (Ribeiro and Lage, 2008). However, a better understanding of the hydrate formation and dissociation mechanism is required for both the design and optimisation of separation processes involving hydrate equilibrium and the understanding of natural gas hydrate formation, accumulation and destabilisation in nature.

For naturally-occurring hydrates, the gases originate either from biogenic or thermogenic sources (Kvenvolden, 1995). Biogenic gases are microbial transformation products which consist of almost exclusively of methane. Thermogenic gases usually come from deep-petroleum reservoirs and although the methane is overwhelmingly represented in those gases, the fraction of C_2-C_5 hydrocarbons is very significant (Bourry et al., 2009; Kida et al., 2006; Milkov et al., 2005; Ruffine et al.). In the case of hydrates from thermogenic gases, the monitoring of the change in the vapour phase composition during that process is particularly interesting since it provides valuable insight into the mechanism of the reaction (Hester et al., 2007; Kumar et al., 2006).

Furthermore, the production of natural gas from naturally-occurring hydrates is now being seriously considered by the gas and petroleum industry, and one of the possible option is to couple the production with the sequestration of carbon dioxide (Goel, 2006). The development of the appropriate technology requires a sufficient knowledge of the mechanical, physical and chemical behaviours of hydrates of both carbon dioxide and natural gas, their mixture as well as their interaction with the sediments. Last but not least, the effects of the gas when being released on the surrounding marine fauna are also of great importance.

On the other hand, carbon dioxide is naturally venting as bubbles and/or in the liquid state to the seafloor at several hydrothermal systems (Inagaki et al., 2006; Lupton et al., 2008). The possible coexistence of carbon dioxide in the liquid, gas and hydrate phase in some hydrothermal sites has already been discovered or proposed (Konno et al., 2006; Nealson, 2006). Therefore, it is important to gather as much information as possible on both natural gas and carbon dioxide hydrates in order to develop appropriate models which enable the description of the behaviour of such fluids within the seafloor or the marine sediments.

The focus of this paper is to describe the new apparatus. Subsequently, the hydrate formation and destabilisation of two different systems involving either carbon dioxide or thermogenic-like gases is investigated.

2 Experimental

2.1 Description of the apparatus

Although many apparatuses have previously been developed to study the properties of gas hydrates ((Sloan and Koh, 2007), there is still a need for developing equipment which incorporates either new features or a combination of features adopted from the literature. In fact, the investigation of gas hydrates in laboratory involves a variety of set-up differing from each other by the properties measured and the analytical techniques used. The most commonly encountered experimental devices are composed of a batch reactor endowed with a stirrer, as well as gas sampling and visual observation systems (Lee et al., 2005; Pic et al., 2001). They are usually used for kinetics and phase equilibrium measurements. Another type of apparatus is custom-made equipment or modified analytical instruments for the measurements of structural and physical properties of gas hydrates such as Raman spectroscopy (Chazallon et al., 2007; Nakano et al., 1998; Sum et al., 1997; Uchida et al., 1995), X-Ray measurements (Bourry et al., 2007; Huo et al., 2005; Seo and Lee, 2004) and NMR spectroscopy (Fleyfel et al., 1994; Seo and Lee, 2004; Subramanian et al., 2000). Both kinds of apparatus previously mentioned enable the study of pure gas hydrates. Beside, there are laboratory facilities for investigating the properties of gas hydrate-bearing sediments or gas hydrates in porous media (Anderson et al., 2003; Eaton et al., 2007; Lee et al., 2002; Madden et al., 2009; Phelps et al., 2001; Waite et al., 2008; Winters et al., 2007). The apparatus presented here was developed keeping in mind the primary features required for an apparatus devoted to the study formation, accumulation and destabilisation of gas hydrate at the macroscopic level. However, incorporating features that would provide versatility in its use and thus enabling possible the investigation on gas hydrates at the mesoscopic level by means of sensors have been incorporated additionally (Sloan and Koh, 2007).

Therefore, the priority for developing this apparatus was to build a system as flexible as possible and allowing for the determination of hydrate-involving phase equilibria and hydrate phase properties as well as the measurement of the kinetics of the hydrate formation and destabilisation processes. It has been designed and constructed to comply with the following requirements:

- It should be possible to investigate on thermogenic-like gases containing or not acid gases, water, brine and carbon dioxide in either the gas, liquid or supercritical state
- It should be possible to monitor the hydrate formation and destabilisation processes, with or without sediment
- Visualisation of the presence of gas hydrate and its morphology within the cell is necessary
- It should be possible to incorporate custom-made sensors to study specific properties of gas hydrates
- Connection of analytical instruments should be possible
- The range of temperature and pressure should cover most of the range of conditions for gas hydrate-involving processes on the continental margins and the polar regions.

Makogon(Makogon, 1997) has also developed an apparatus for kinetic and phase equilibrium measurements which has several similarities with our developed one. Its apparatus has several windows for visual observation and filming activity. With a volume of the reaction chamber more the 15 time bigger than ours, it was also possible to perform static and dynamic experiment at pressure up to 20 MPa. However this new apparatus aims at enabling us to work at pressure up to 60 MPa, and being easily implemented with analytical instruments and / or custom-made sensors. Thus, some particular properties of hydrates could be investigated without making to much modification on the set-up.

A schematic diagram of the apparatus is shown in figure 1. The main component of the apparatus consists of a high-pressure view cell which was constructed from type 316-Ti stainless steel. The reaction chamber is a cylindrical cavity of 25.5 mm diameter. The volume of the cell can be varied by displacement of a 17-4 PH made piston which is housed in a piston assembly, which latter is attached to one end of the cell. The piston is sealed against the wall of the cell with a SITEC home-made packing assembly consisting of two bushings (316 L stainless steel and PFTE respectively), two O-rings (PTFE and viton respectively), a PTFE lip seal and a PTFE/ 25 % Kohle seal ring. The construction of the piston and the cell assembly allows for the cell volume to be reduced by a third at of the maximum cell volume at full displacement of the piston, and therefore a compression ratio of 3:1 can be achieved. Based on the design of Ruffine and Trusler (2009), the cell was equipped with a pair of 12 mm diameter ports (one located at the top and one at the bottom) which can be used to accommodate sensors for either in-situ hydrate property measurements or compositional analysis of the fluid phases. In order to allow for the visualisation of chemical reaction and/or phase equilibrium, the cell was also closed at each end by two sapphire window units: a small sapphire window of 15 mm diameter and 10 mm thickness which seals the threaded end of the piston shaft (using an optical fibre enabling illumination from the backside), and a larger unit at the front end with a sapphire window of 38 mm diameter and 14 mm thickness housed in a AISI 660 high alloyed steel cap (for visual observation or Raman spectroscopy analysis). This latter window unit has a special SITEC home-made sealing system using PTFE gaskets and a 316-L annular ring, allowing for the whole unit to be removed easily, and thus for harvesting gas hydrate samples while keeping its decomposition as low as possible. Alternatively, this window unit can be replaced by a different one equipped with additional sensor ports. The cell was also fitted with four high-pressure fluid ports that accepted 6.35 mm o.d. conned-and-threaded tubing. Three of these ports were used for connection to the pressure transducer, the temperature probe and the relief valve, respectively, whereas the fourth one was used for fluid injection.

For thermoregulation purposes, the cell was housed in a welded metal jacket enabling thermal fluid to circulate around the cell by means of two 9.53 mm Gas-connection with a temperature being kept constant to within ±0.2 K. The dead volume in the high-pressure cell and in all fittings were minimised by the use of fittings that either eliminated or had the smallest possible value.

As indicated in figure 1, several analytical instruments or sensors can be connected to the high-pressure cell. Hydrate structural analysis and phase-transition kinetic measurements can be performed by means of a benchtop Raman spectrometer (Advantage 532 from DeltaNu, USA) with a frequency doubled Nd:YAG laser beam at the 532 nm line. The latter was connected to the large sapphire-window unit endowed with input optic extensions having objectives incorporated to extend the exit beam and to enable receiving the collection signals 10, 20 or 30 mm beyond the window. The resolution of this instrument is within ±10 cm^{-1}. If necessary, the Raman spectrometer can be replaced by a camera connected to a computer for capturing the process under study. For molecular composition analysis, samples can be taken from either the upper phase or the lower phase (usually a fluid phase) and analyzed by gas chromatography. To do so, small amounts of the substances are directly injected into the carrier gas stream of a gas chromatograph coupled with quadrupole mass spectrometer detector (GC-MS) using an electrically driven micro sampler ROLSI developed at Ecole des Mines de Paris (Guilbot et al., 2000). The chromatograph is a 7890A Agilent gas chromatograph coupled with an Agilent 5975C quadruple mass spectrometer detector. It is a custom-made instrument, equipped with a TCD-FID-mass detector and two capillary columns, Pora PLOT Q and molecular sieve, which can be put in series for the analysis of both hydrocarbons and permanent gases like nitrogen and oxygen.

A vacuum pump was also connected to the high-pressure cell, which serves for its evacuation. The temperature inside the cell chamber is measured with a K-type thermocouple, calibrated on the basis of the ITS-90 with an accuracy of ±0.4 K. The pressure inside the cell is measured with S-10 WIKA pressure transmitter, calibrated using an oil pressure balance DH N° 6114/6115 with an accuracy of ±0.01 MPa. Both sensor calibrations were carried out at the Laboratoire National de Métrologie et d’Essais (LNE), France. Temperature regulation of the cell was achieved with a refrigerated/heating circulator bath (Ministat 230 from Huber) using silicon oil M40.165.10 from Huber. Continuous monitoring of both temperature and pressure profiles of the hydrate processes as a function of time was possible using an Eurotherm Chessell 6100 paperless graphic recorder. A computer containing the appropriate software was used for the acquisition of both Raman spectroscopy and gas chromatography data.

The apparatus has an operating temperature range from 253 K to 473 K, for a maximum working pressure of 60 MPa. Gas was injected into the cell either directly from a cylinder at pressures up to 20 MPa or by means of a F-210CV mass flow controller from Bronkhost High-Tech, which can be used up to 10 MPa. Liquid was injected with a high-pressure liquid metering pump from Eldex at pressures up to 52.5 MPa.

2.2 Calibrations

Apparatus volume

This equipment is also suitable for *pvT* measurements on gas hydrates or on the phase behaviour of the hydrate-forming fluids. Therefore, the combined volume of the cell, fitting and relief line was needed for determining the initial amounts of gas from measurements of temperature and pressure. In order to determine this quantity, the initially evacuated system was filled with degassed and deionised water at a thermostated temperature of 298 K using the liquid metering pump, and brought into equilibrium at a pressure of 0.5 MPa. The assembly -water + bottle + tubing- was weighted before and after each injection. Thus the mass of the quantity of water that completely filled the apparatus at T = 298 K and p = 0.5 MPa was determined. From that mass, the exact inner volume could be determine by means of the density of pure water taken from the NIST database. The relative uncertainty on the liquid water density was given as 0.001 %. The calibration of the relief valve as well as the pressure transducer was determined separately. The calibration was repeated three times for the system at zero, half and full volume compression. The volumes obtained were (65.43 ± 0.3) cm^3, (42.89 ± 0.8) cm^3 and (20.79 ± 0.6) cm^3 respectively.

Chromatograph

The response of both the FID and TCD was calibrated using a commercially-prepared synthetic natural gas mixture from L’Air Liquide. Considering the reproducibility of gas chromatography and the uncertainty in calibration, we estimated the accuracy in the composition measurements to be within ± 3 % of the molar fraction. The analysis was performed at a temperature program running from 313.15 K to 503.15 K. A Pora PLOT Q column was taken for separation and helium was used as a carrier gas. The TCD and FID were used for quantitative analysis while the mass spectrometer was used for the purpose of verification of the compounds. The NIST05 library was used for identification of the substances. In the series of measurements performed in this study, due to the complexity of the mixture, the calibrations and quantifications were carried out for the hydrocarbons only.

2.3 Materials

The deionised water has been degassed before using by boiling. The gases were directly used as received without further purification. Methane and carbon dioxide were purchased from Alpha Gaz with a specified minimum purity of 99.995 % for both. The synthetic natural gas mixture used in this study was purchased from L'Air Liquide. Its composition is presented in table 1 along with its uncertainty in terms of the molar percentage.

2.4 Procedure

The procedure used for hydrate formation and destabilisation depends deeply on the system under investigation. Here, two different procedures have been used.

Injection of water into liquid CO_2

After evacuation of the apparatus, carbon dioxide is injected as a gas phase at 298 K. The system was left 3 hours to reach equilibrium. After this period of time, the pressure, temperature and volume were taken. Thus, knowing the compressibility factor and the T-p condition, the exact amount of CO_2 injected into the cell can be calculated. The system was then brought to 275.63 K to liquefy a fraction of the loaded gas. It is worth to notice, that knowing the molar volume of both the liquid and gas phases, it is also possible to determine the fraction of the gas being liquefied. Finally, water was injected into the liquefied fraction of CO_2 using the metering liquid pump at a flow rate of 0.5 mL/min. The injection was stopped when the pressure of the system, initially equal to 3.70 MPa which is very close to the vapour pressure of CO_2 at 275.63 K, started increasing by more than 0.1 MPa. We assumed that the increase of the pressure starts when reaching the maximum amount of hydrate that can be formed. From that point, there is no liquid CO_2 to react with the injected water. Therefore after that point the injected water will serve for dissociation of the hydrate. This assumption can be justified by taking a look at figure 2. One can see that the liquid level does not change during the hydrate growth on the pictures a, b and c. That means that the liquid uptake by the formation of the hydrate is replaced by the liquefaction of an equivalent amount of gas. Thus, the hydrate will grow until all the CO_2 has been transformed into liquid, then the liquid level will decrease until vanishing at constant pressure. Then, the injection of water will only increase the pressure.

Thus, after the increase of the pressure, water was injected once again while expanding the cell volume to its full capacity and keeping the pressure at 3.80 MPa. Then, the system was left for hydrate dissolution. The system (water + bottle + tubing) was weighted before and after each injection to determine the exact amount of water.

The cell was initially loaded with 0.120 mol of CO_2. The amount of water injected before the increase of the pressure was 0.658 mol. The ratio of those values is 5.46, corresponding to a hydration number which is lower than the respective hydration numbers reported in the literature (Anderson, 2003). This is in accordance with the fact that part of the CO_2 will be dissolved into the water to saturate it before the hydrate formation will be initiated.

The amount of water injected after the increase of the pressure for the dissolution of the hydrates was 2.312 mol.

Hydrate formation and decomposition using a cooling / heating process

Before each experiment, the temperature was fixed and kept constant at its initial value, then the apparatus was evacuated and purged with the gas to be investigated.

In the case of the thermogenic-like gas mixture studied here, the preparation of the mixture was made from the commercially-available natural gas mixture and pure methane. Thus, the gas mixture was at first loaded into the high-pressure cell at its maximum volume, following the addition of methane until a pre-determined pressure was attained. The knowledge of the temperature, pressure, cell volume and compressibility factor of methane enables us to determine the composition of the final gas mixture. This starting composition was also verified by gas chromatography. A good agreement between both *pvT* and chromatographic methods was obtained. A pre-determined volume of water was subsequently injected into the cell using the metering liquid pump. In a second step, the system (water + thermogenic-like gases) is compressed until a set pressure was reached.

Finally the cooling/heating-cycle method was applied to study the hydrate formation and dissociation. For this purpose, a stepwise procedure was used, whereby the temperature was lowered by 2.5 K quickly, and then kept constant for 4hours. This was repeated until the temperature of 268 K has been reached. The analysis of the vapour phase was always performed at the end of the steps. Temperature and pressure were recorded every hour, thus, the *p*, *T*-trace could be drawn.

3 Results and discussion

3.1 Hydrate formation by injection of a water droplet into liquid CO_2

The hydrate formation and dissolution processes of CO_2 hydrates have been studied by injecting water into liquid CO_2. The knowledge of the characteristics of such a system is very important because it can provide useful information of the behaviour of liquid CO_2 venting in sedimented-hydrothermal systems from its location of production near the mantle, then its migration through the sediment to the seafloor. The experimental hydrate-formation process was captured using a camera and monitored by means of Raman spectroscopy. The formation process is illustrated in figure 2. Picture (a) shows a water droplet injected into the liquid CO_2. The hydrate nucleation and growth took less than 5 minutes. One can already see some hydrate crystals that have been formed at the bottom of the water droplet. This reveals that the nucleation has started at the metal-water-CO_2 contact interface, then propagated upwards into the droplet as can be seen on pictures (b) and (c). Finally, the entire cell is filled with hydrates as becomes evident from picture (d).

Figure 3 represents the Raman spectra obtained for the CO_2 molecules as occurring in the gas and the liquid state, respectively, and after injection of water into the liquid CO_2. For the latter case, the Raman beam was focused towards the water droplet. The Raman peaks of the CO_2 molecules in the different phases, i.e. the liquid, the hydrate after 30 min and the vapour phase. were 1281 and 1387 cm^{-1}, 1277 and 1382 cm^{-1} and 1286 and 1389 cm^{-1} respectively. These values are found to be in agreement with literature values, although our values for the CO_2 present in the liquid and the hydrate, respectively, were 1 cm^{-1} higher than the corresponding values from the literature (Nakano et al., 1998; Sloan and Koh, 2007; Uchida et al., 1995). The Raman peaks of the CO_2 molecules in the mixture after 3 min. were 1282 and 1386 cm^{-1}. They are very close to the values for the liquid CO_2, but with an intensity much more smaller. Furthermore, when analysing the host water-molecule bands in figure 4 one can realise that its intensity attenuates with time during the hydrate growth process in the liquid CO_2. The peak of pure water was determined by injecting water into the cell at 275.63 K and 3.70 MPa which were the conditions under which the hydrate formation took place. Its value of 3190 cm^{-1} was in agreement with the corresponding value from the literature (Schicks et al., 2005). Therefore, from the above observations, one hypothesis that could be drawn from these measurements is that the Raman spectrum at 3 min is a transition state in which both water and CO_2 molecules form a structure close to the final hydrate structure. This structure is possibly similar in terms of the arrangement of the molecules. However, it differ with regard to the interactions between molecules.

Water has been injected into the system in order to monitor the kinetics of the isochoric process of the dissolution of the hydrates. Figure 5 represents the evolution of the pressure as a function of time. Two distinct regions represented by A and B can be identified. The region A, corresponding to a decrease in pressure up to 1.76 MPa, represents the dissolution of the hydrates. The region B, where the pressure has reached a steady state, indicates the end of the hydrate dissolution process. For that case, the dissolution took about 87 hours. However, the visual observation allowed us to detect some hydrates having remained in the cell, surrounded with liquid water. We could not observe visually the presence of a vapour phase leading to the dissociation of the hydrates instead of their dissolution. Thus, in this case, the amount of injected water was not sufficient to allow for a complete dissolution of the hydrate. In the view of this result, the implementation of a back pressure regulator on the apparatus is desirable in the future, as this will enable the investigation of the hydrate dissolution process at constant pressure to simulate the condition of constant pressure encountered at the seafloor for instance. With such a configuration, water could be injected continuously using the metering pump until complete hydrate dissolution. The amount of water used will be determined by weighting before and after the experiment.

3.2 Hydrate formation and dissociation of a thermogenic-like gas mixture

The formation and dissociation processes of complex natural gas-like hydrate have been studied during isochoric cooling and heating. The molecular composition of the natural gas-like mixture is given in table 2. The p, T-trace has been drawn for this mixture and is shown in figure 6. The evolution of the pressure as well as the propane composition in the vapour phase as a function of time is illustrated in figure 7.

After compression, the system is at point A (T= 293.25 K and p=8.21 MPa). During cooling of the system, hydrate formation has started at point B (T=278.45 K and p=7.59 MPa) at a supercooling of approximately 14 K, which corresponds to 27 hours of experiment from figure 7. A pressure drop of 1.4 MPa is observed in less than two hours as can be seen in figure 7 (and represented by the segment BC' in figure 6). This visually corresponds to the formation of a hydrate layer (or skin) at the vapour/liquid interface. The temperature keeps decreasing stepwise until point C (T=267 K and p=5.47 MPa) is reached, while the pressure tends to stabilise from C' at T=274.05 K and p=5.67 MPa. The hydrate layer formed at the vapour/liquid interface hinders the diffusion of the gas into the liquid, and therefore limits considerably any further hydrate formation as can be seen in figure 7 (the segment CC' is almost horizontal). This phenomenon and similar ones were also observed by Hester et al. and Osegovic et al. (Hester et al., 2007; Osegovic et al., 2007).

Once the temperature of 267 K has been reached we have carefully cracked the hydrate skin by slightly compressing the system by an additional increment of 0.3 MPa, after we have returned to the original pressure of 5.47 MPa. This operation was carried out in less than half minute. Straight after this cracking, we observed a new pressure drop of 1.5 MPa in less than half hour, leading the system to point D at T=267.25 K and p=3.97 MPa. This experiment highlights the importance of the hydrate skin which acts almost as a barrier, and the consequence of breaking that barrier on the kinetics of the hydrate formation in a closed system. Such a behaviour needs to be taken into consideration when developing any kind of hydrate-based technology for natural gas transportation and storage, as well as for separation processes. This behaviour can also be encountered during hydrate formation within sediments, and might explain the presence of free gas within the gas hydrate stability zone (GHSZ). In fact, due to the heterogeneity of the sediment and its interconnected pore web, pocket-like structures can occur like veins. These structures can be isolated from others structures. Thus, they can act as traps in which water and free gas can be in contact. Thus, those structures can show different degrees of hydrate saturation, a phenomenon which probably depends on their geometry. The latter can more or less promote gas/water contact, and therefore promote the accumulation of hydrates. However, this remains a hypothetic pathway for the hydrate distribution within sediments and, hence, will need further investigations. There was a probability of forming ice since the system was brought to temperature below the ice point. However, by visual observation we did not notice ice formation, neither on the wall of the cell chamber, nor underneath the hydrate skin. Accordingly, even if ice formation had occurred, that should have happened to a very small amount compares to the hydrate skin.

The system has been kept at 267 K for four hours before the stepwise heating process was started. The section (CC') and (DE) are almost parallel, which corresponds to a step when the hydrates are heated without dissociation. On the section (EF), active hydrate dissociation took place. The dissociation is completed at point F (T=288.55 K and p=7.77 MPa) which is the hydrate equilibrium point. Section (FG) represents the thermal expansion of both the liquid and gas phases in equilibrium.

The change in the vapour phase composition has been monitored during the hydrate formation process. Vapour phase composition measurements have been carried out after 0, 4, 8, 16, 24, 28, 32 and 36 hours of the experiment. Only the normalized hydrocarbon compositions were measured and shown because of some difficulties that have arisen upon trying to correctly separate nitrogen and carbon dioxide with the hydrocarbons on the Pora PLOT Q column. Gas composition measurements were stopped after 36 hours of the experiment because, even if the vapour phase was visually detected around the capillary of the ROLSI sampler, the later has been plugged by hydrate crystals, making the vapour phase sampling not reliable. Table 3 summarises the measured vapour phase composition at the eight different times. As mentioned previously, hydrate formation started after the experiment has been running for 27 hours. The composition of the thermogenic-like gases is diagnostic of structure II hydrate (Sloan and Koh, 2007). The change in composition of all hydrocarbons during the observation time from time 0 to 4h is due to the compression of the system, involving the dissolution of the species in the water as a function of their solubility. In the following, we took the propane as compound of reference for it is, like the isobutane, a structure II driven-molecule. Figure 7 illustrates the evolution of the propane mole fraction in the vapour phase with time. After an important drop caused by dissolution due to compression, the propane mole fraction slightly increases, then decreases again slowly up to the hydrate formation point. At the hydrate formation point the decrease is more abrupt, corresponding to the enclathration of that molecule. A similar trend is observed for both isobutane and ethane (figure 9 and 10). The methane composition of the vapour phase increases in the vapour phase; its trend being nearly symmetrically opposed to this of propane (figure 8). This observation is in agreement with the results of Hester et al. (Hester et al., 2007), and consistent with the preferential enclathration of propane and isobutane during the formation of structure II hydrate. The relative depletion of the mole fraction of ethane, propane and isobutane in the vapour phase is 11.51 %, 21.19 % and 20.61 %, respectively. The similar behaviour of propane and isobutane let us conclude that both molecules are enclathrated in a similar proportion in the hydrate crystal. However, owing to the complexity of our mixture, this has to be verified by monitoring the change in the vapour phase composition during hydrate formation for a binary gas mixture involving propane and isobutane.

4 Conclusion

In order to achieve an appropriate description and understanding of the behaviour of gas hydrate formation and destabilisation in nature as well as in new industrial processes, laboratory experiments on their formation, accumulation and destabilisation are key issues. Those experiments, along with field data are necessary to evaluate the fate of gas hydrate-bearing sediments on continental margins, the injection of CO_2 into gas hydrate reservoirs if this sequestration scheme is chosen in the future and the CO_2 venting from hydrothermal sources. In the present work, a novel high-pressure apparatus devoted to gas hydrate investigations has been fully described. It enables the study of all processes mentioned above. Experimental thermodynamics and kinetics data on those processes have been generated for pure CO_2 and a thermogenic-like gas. The data presented in this work provide some insight into the processes involved in the formation, dissociation and dissolution of gas hydrates. In order to get closer to the actual conditions when studying gas hydrate destabilisation, the present apparatus will be improved in the future by implementing a back pressure regulator to simulate the constant pressure of the seafloor. Although this work does not include systems containing sediments, the present apparatus does offer the possibility of integrating sediment in order to study gas hydrate-bearing sediments. Such investigations are desirable as they complement the data on pure hydrates. This will be the topic of a future work.

References

Anderson, G.K., 2003. Enthalpy of dissociation and hydration number of carbon dioxide hydrate from the Clapeyron equation. Journal of Chemical Thermodynamics, 35(7): 1171-1183.

Anderson, R., Llamedo, M., Tohidi, B. and Burgass, R., 2003. Experimental measurement of methane and carbon dioxide clathrate hydrate equilibria in mesoporous silica. J. Phys. Chem. B, 107(15): 3507-3514.

Bourry, C. et al., 2007. X-ray synchrotron diffraction study of natural gas hydrates from African margin. Geophysical Research Letters, 34(22).

Bourry, C. et al., 2009. Free gas and gas hydrates from the Sea of Marmara, Turkey Chemical and structural characterization. Chemical Geology, 264(1-4): 197-206.

Briaud, J. and Chaouch, A., 1999. Hydrate melting in soil around hot conductor. Journal of Geotechnical and Geoenvironmental Engineering, 123(7): 645.

Chazallon, B., Focsa, C., Charlou, J.L., Bourry, C. and Donval, J.P., 2007. A comparative Raman spectroscopic study of natural gas hydrates collected at different geological sites. Chemical Geology, 244: 175-185.

Collet, T. and Kuuskraa, V., 1998. Hydrates contain vast store of world gas resources. Oil & gas journal, 96(19): 90-95.

Duc, N.H., Chauvy, F. and Herri, J.M., 2007. CO2 capture by hydrate crystallization - A potential solution for gas emission of steelmaking industry. Energy Conversion and Management, 48(4): 1313-1322.

Eaton, M., Mahajan, D. and Flood, R., 2007. A novel high-pressure apparatus to study hydrate–sediment interactions. Journal of Petroleum Science and Engineering, 56(1-3): 101-107.

Englezos, P. and Lee, J., 2005. Gas hydrates: A cleaner source of energy and opportunity for innovative technologies. Korean Journal of Chemical Engineering, 22(5): 671-681.

Fleyfel, F., Song, K.Y., Kook, A., Martin, R. and Kobayashi, R., 1994. C-13 NMR of hydrate precursors in metastable regions. International Conference on Natural Gas Hydrates, 715: 212-224.

Goel, N., 2006. In situ methane hydrate dissociation with carbon dioxide sequestration: Current knowledge and issues. Journal of Petroleum Science and Engineering, 51(3-4): 169-184.

Guilbot, P., Valtz, A., Legendre, H. and Richon, D., 2000. Rapid on-line sampler-injector: a reliable tool for HT-HP sampling and on-line GC analysis. Analusis, 28(5): 426-431.

Hammerschmidt, E., 1934. Formation of gas hydrates in natural gas transmission lines. Industrial & Engineering Chemistry, 26(8): 851-855.

Hester, K. et al., 2007. Direct measurements of multi-component hydrates on the seafloor: Pathways to growth. Fluid Phase Equilibria, 261(1-2): 396-406.

House, K.Z., Schrag, D.P., Harvey, C.F. and Lackner, K.S., 2006. Permanent carbon dioxide storage in deep-sea sediments. Proceedings of the National Academy of Sciences of the United States of America, 103(33): 12291-12295.

Huo, Z., Eaton, M., Miller, K.T. and Sloan, E.D., 2005. Design and construction of an X-ray diffraction cell for hydrate studies at elevated pressures. International Journal of Thermophysics, 26(1): 107-114.

Inagaki, F. et al., 2006. Microbial community in a sediment-hosted CO2 lake of the southern Okinawa Trough hydrothermal system. Proceedings of the National Academy of Sciences of the United States of America, 103(38): 14164-14169.

Kida, M. et al., 2006. Coexistence of structure I and II gas hydrates in Lake Baikal suggesting gas sources from microbial and thermogenic origin.

Konno, U. et al., 2006. Liquid CO2 venting on the seafloor: Yonaguni knoll IV hydrothermal system, Okinawa Trough. Geophysical Research Letters, 33(16).

Kumar, R., Wu, H. and Englezos, P., 2006. Incipient hydrate phase equilibrium for gas mixtures containing hydrogen, carbon dioxide and propane. Fluid Phase Equilibria, 244(2): 167-171.

Kvenvolden, K., 1995. A review of the geochemistry of methane in natural gas hydrate. Organic Geochemistry, 23(11-12): 997-1008.

Kwon, T., Kim, H. and Cho, G., 2008. Dissociation Behavior of CO2 Hydrate in Sediments during Isochoric Heating. Environmental Science & Technology, 42(22): 8571-8577.

Lee, J.D., Susilo, R. and Englezos, P., 2005. Kinetics of structure H gas hydrate. Energy & Fuels, 19(3): 1008-1015.

Lee, K., Lee, H., Lee, J. and Kang, J., 2002. CO2 hydrate behavior in the deep ocean sediments; phase equilibrium, formation kinetics, and solubility. Geophysical Research Letters, 29(21): 2034.

Li, S., Fan, S., Wang, J., Lang, X. and Liang, D., 2009. CO2 capture from binary mixture via forming hydrate with the help of tetra-n-butyl ammonium bromide. Journal of Natural Gas Chemistry, 18(1): 15-20.

Linga, P., Adeyemo, A. and Englezos, P., 2008. Medium-pressure clathrate hydrate/membrane hybrid process for postcombustion capture of carbon dioxide. Environmental Science & Technology, 42(1): 315-320.

Lupton, J. et al., 2008. Venting of a separate CO2-rich gas phase from submarine arc volcanoes: Examples from the Mariana and Tonga-Kermadec arcs. Journal of Geophysical Research-Solid Earth, 113(B8).

Madden, M., Ulrich, S., Szymcek, P., McCallum, S. and Phelps, T., 2009. Experimental formation of massive hydrate deposits from accumulation of CH4 gas bubbles within synthetic and natural sediments. Marine and Petroleum Geology, 26(3): 369-378.

Makogon, Y., 1997. Hydrates of hydrocarbons. Pennwell Publishing Company, Tulsa, Oklahoma, 482 p.

Makogon, Y., Holditch, S. and Makogon, T., 2007. Natural gas-hydrates—A potential energy source for the 21st Century. Journal of Petroleum Science and Engineering, 56(1-3): 14-31.

Max, M., 2003. Natural gas hydrate: in oceanic and permafrost environments. Kluwer Academic Pub.

Max, M., Johnson, A. and Dillon, W., 2006. Economic geology of natural gas hydrate. Kluwer Academic Pub.

Milkov, A., Claypool, G., Lee, Y. and Sassen, R., 2005. Gas hydrate systems at Hydrate Ridge offshore Oregon inferred from molecular and isotopic properties of hydrate-bound and void gases. Geochimica et Cosmochimica Acta, 69(4): 1007-1026.

Milkov, A. and Sassen, R., 2002. Economic geology of offshore gas hydrate accumulations and provinces. Marine and Petroleum Geology, 19(1): 1-11.

Moridis, G.J., 2003. Numerical studies of gas production from methane hydrates. Spe Journal, 8(4): 359-370.

Moridis, G.J. et al., 2009. Toward Production From Gas Hydrates: Current Status, Assessment of Resources, and Simulation-Based Evaluation of Technology and Potential. Spe Reservoir Evaluation & Engineering, 12(5): 745-771.

Moridis, G.J. et al., 2004. Numerical studies of gas production from several CH4 hydrate zones at the Mallik site, Mackenzie Delta, Canada. Journal of Petroleum Science and Engineering, 43(3-4): 219-238.

Moridis, G.J. and Sloan, E.D., 2007. Gas production potential of disperse low-saturation hydrate accumulations in oceanic sediments. Energy Conversion and Management, 48(6): 1834-1849.

Nakano, S., Moritoki, M. and Ohgaki, K., 1998. High-pressure phase equilibrium and Raman microprobe spectroscopic studies on the CO2 hydrate system. Journal of Chemical and Engineering Data, 43(5): 807-810.

Nealson, K., 2006. Lakes of liquid CO2 in the deep sea. Proceedings of the National Academy of Sciences of the United States of America, 103(38): 13903-13904.

Osegovic, J., Tatro, S., Holman, S., Ames, A. and Max, M., 2007. Growth kinetics of ethane hydrate from a seawater solution at an ethane gas interface. Journal of Petroleum Science and Engineering, 56(1-3): 42-46.

Phelps, T.J. et al., 2001. A new experimental facility for investigating the formation and properties of gas hydrates under simulated seafloor conditions. Review of Scientific Instruments, 72(2): 1514-1521.

Pic, J.S., Herri, J.M. and Cournil, M., 2001. Experimental influence of kinetic inhibitors on methane hydrate particle size distribution during batch crystallization in water. Canadian Journal of Chemical Engineering, 79(3): 374-383.

Purwanto, Y.A., Oshita, S., Seo, Y. and Kawagoe, Y., 2001. Concentration of liquid foods by the use of gas hydrate. Journal of Food Engineering, 47(2): 133-138.

Ribeiro, C. and Lage, P., 2008. Modelling of hydrate formation kinetics: State-of-the-art and future directions. Chemical Engineering Science, 63(8): 2007-2034.

Ruffine, L. et al., Formation history of the gas hydrates from the Sea of Marmara. Part I: Origin of the hydrates forming-gases. Chemical Geology, submitted.

Ruffine, L. and Trusler, J.P.M., 2009. Phase behaviour of mixed-gas hydrate systems containing carbon dioxide. The Journal of Chemical Thermodynamics, In Press, doi:10.1016/j.jct.2009.11.019.

Schicks, J.M., Erzinger, J. and Ziemann, M.A., 2005. Raman spectra of gas hydrates - differences and analogies to ice 1h and (gas saturated) water. Spectrochimica Acta Part a-Molecular and Biomolecular Spectroscopy, 61(10): 2399-2403.

Seo, Y.T. and Lee, H., 2004. Structure and guest distribution of the mixed carbon dioxide and nitrogen hydrates as revealed by X-ray diffraction and C-13 NMR spectroscopy. Journal of Physical Chemistry B, 108(2): 530-534.

Sloan, E. and Koh, C., 2007. Clathrate hydrates of natural gases. CRC Press.

Subramanian, S., Kini, R.A., Dec, S.F. and Sloan, E.D., 2000. Evidence of structure II hydrate formation from methane plus ethane mixtures. Chemical Engineering Science, 55(11): 1981-1999.

Sum, A.K., Burruss, R.C. and Sloan, E.D., 1997. Measurement of clathrate hydrates via Raman spectroscopy. Journal of Physical Chemistry B, 101(38): 7371-7377.

Torres, M. et al., 2008. Methane hydrate formation in turbidite sediments of northern Cascadia, IODP Expedition 311. Earth and Planetary Science Letters, 271(1-4): 170-180.

Uchida, T., Takagi, A., Kawabata, J., Mae, S. and Hondoh, T., 1995. Raman-spectroscopy analyses on the growth-process of CO2 hydrates. Energy Conversion and Management, 36(6-9): 547-550.

Waite, W.F., Kneafsey, T.J., Winters, W.J. and Mason, D.H., 2008. Physical property changes in hydrate-bearing sediment due to depressurization and subsequent repressurization. Journal of Geophysical Research-Solid Earth, 113(B7).

Walsh, M. et al., 2008. Preliminary report on the economics of gas production from natural gas hydrates.

White, M., 2008. Numerical Simulation of Methane Hydrate Production from Geologic Formations via Carbon Dioxide Injection. OTC 19458.

Winters, W.J., Waite, W.F., Mason, D.H., Gilbert, L.Y. and Pecher, I.A., 2007. Methane gas hydrate effect on sediment acoustic and strength properties. Journal of Petroleum Science and Engineering, 56(1-3): 127-135.

Figure captions

Figure 1 : Schematic diagram of the apparatus : GC-MS, Gas chromatography coupled with Mass spectrometer; Raman spectrometer; TR, Thermal regulator; VP, vacuum pump.

Figure 2 : Hydrate formation process by injecting water into liquid CO_2 : A droplet of water is injected into the liquid CO_2 (picture (a)). The hydrate nucleation starts at the bottom of the cell (picture (b)), then grows upward into the droplet (picture (c)). The injection of more water allows filling the cell with hydrate (picture (d)).

Figure 3 : Raman spectra of the CO_2 molecules in liquid state, vapour state and after injection of water

Figure 4 : Raman spectra of the water molecules in the liquid state and after injecting water into liquid CO_2

Figure 5 : Carbon dioxide hydrate dissolution in water as a function of time

Figure 6 : Synthetic natural-gas hydrate formation and dissociation in water

Figure 7 : Evolution of the pressure and iso-butane molar fraction as a function of time

Figure 8 : Evolution of the methane and iso-butane molar fractions as a function of time

Figure 9 : Evolution of the ethane and iso-butane molar fractions as a function of time

Figure 10 : Evolution of the propane and iso-butane molar fractions as a function of time

Table 1 : Molecular composition of the synthetic natural gas

Components	Mole %	Uncert. %
Ethane	8.43	2
Propane	6.06	2
Isobutane	2.98	2
n-Butane	3.05	2
Isopentane	0.954	3
Neopentane	0.547	3
Carbon dioxide	1.088	2
Nitrogen	3.416	2
n-Hexane	0.502	3
Helium	0.501	3
Methane	QS	

Table 2 : Molecular composition of the thermogenic-like gases

Components	Molar %
Methane	92.89
Ethane	2.18
Propane	1.57
Isobutane	0.77
n-Butane	0.79
Isopentane	0.25
Neopentane	0.14
n-Hexane	0.13
Carbon dioxide	0.28
Nitrogen	0.88
Helium	0.13

Table 3 : Evolution of the hydrocarbon vapour-phase composition (in mole fraction) during the 36 first hours of the experiment.

Components	t = 0 h	t = 4 h	t = 8 h	t = 16 h	t = 24 h	t = 28 h	t=32 h	t = 36 h
Methane	0.9410	0.9470	0.9458	0.9456	0.9465	0.9464	0.9486	0.9500
Ethane	0.0221	0.0216	0.0221	0.0222	0.0220	0.0220	0.0211	0.0195
Propane	0.0159	0.0140	0.0142	0.0143	0.0141	0.0140	0.0134	0.0125
Isobutane	0.0080	0.0069	0.0071	0.0071	0.0071	0.0071	0.0066	0.0063
n-Butane	0.0078	0.0066	0.0068	0.0068	0.0068	0.0067	0.0064	0.0067
Neopentane	0.0025	0.0007	0.0006	0.0005	0.0004	0.0005	0.0007	0.0014
Isopentane	0.0014	0.0012	0.0012	0.0012	0.0011	0.0012	0.0012	0.0014
n-Hexane	0.0013	0.0020	0.0021	0.0021	0.0020	0.0021	0.0020	0.0021

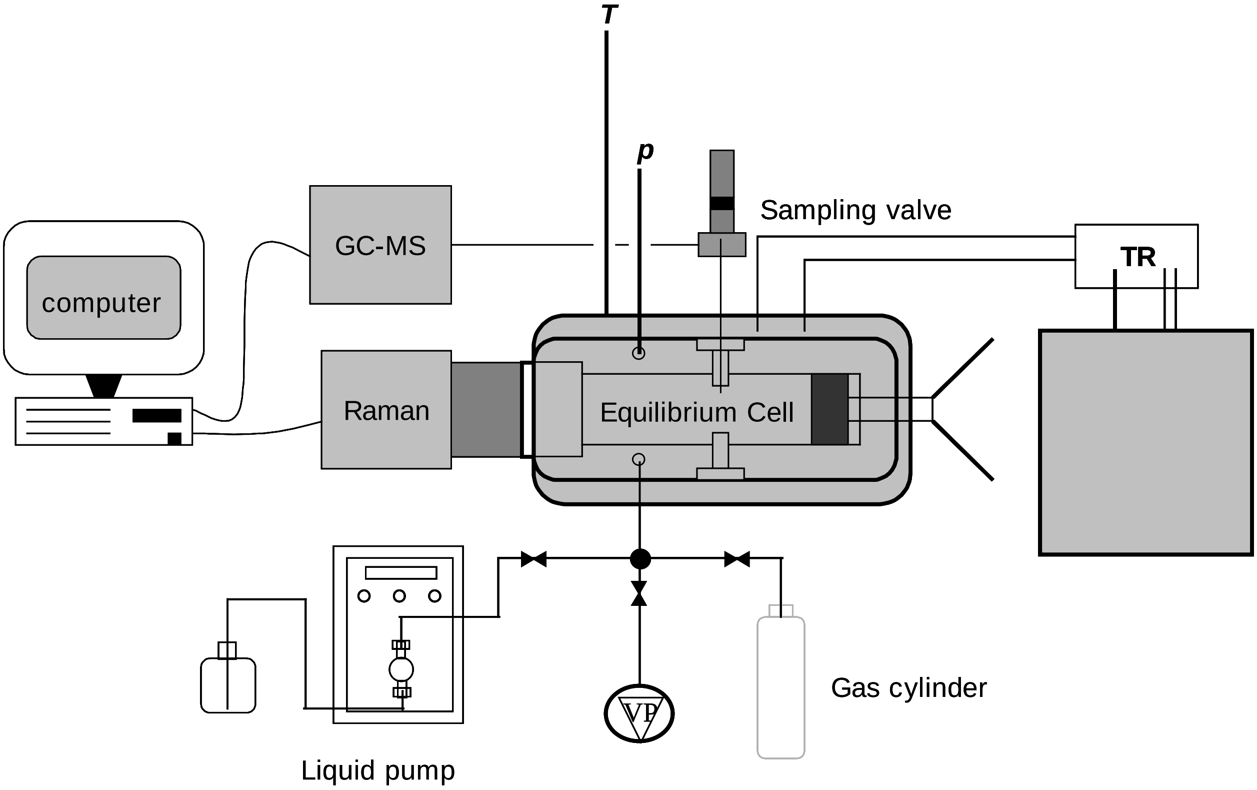
T
p
Sampling valve
GC-MS
TR
computer
Raman
Equilibrium Cell
VP
Gas cylinder
Liquid pump

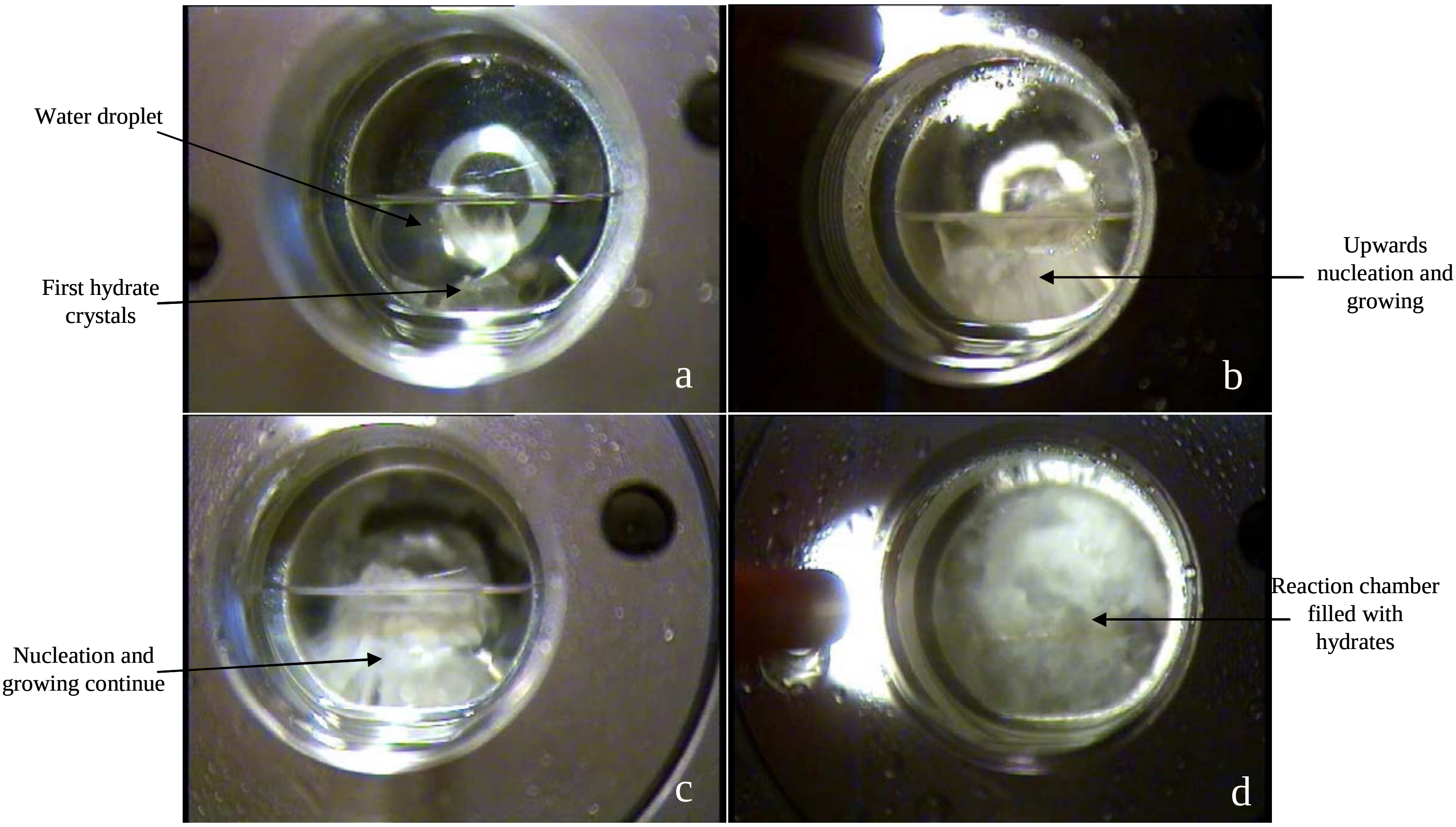
Water droplet
First hydrate crystals
a
Upwards nucleation and growing
b
Nucleation and growing continue
c
Reaction chamber filled with hydrates
d

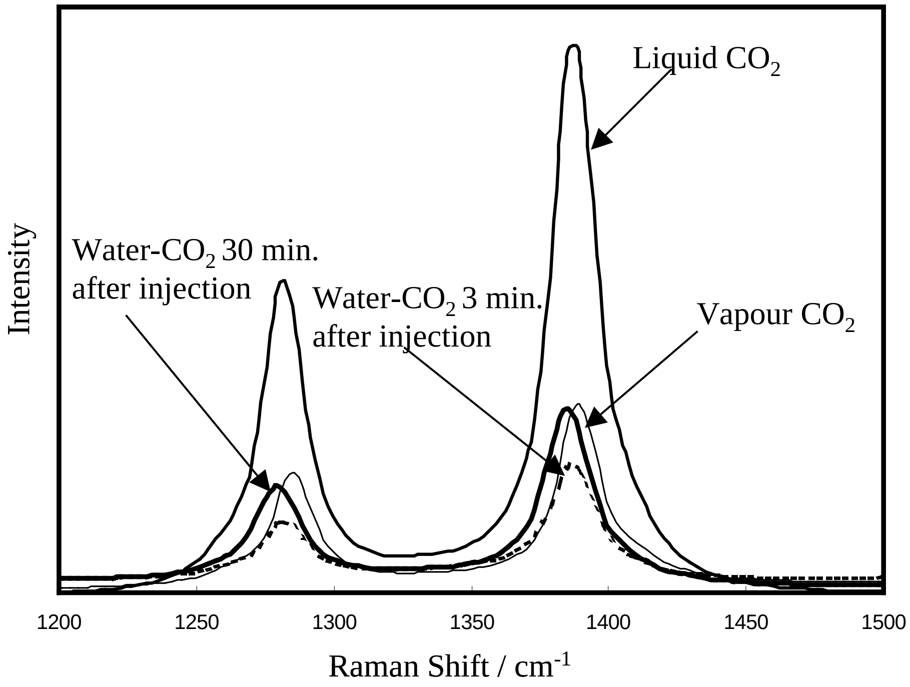
Liquid CO_2
Water-CO_2 30 min. after injection
Water-CO_2 3 min. after injection
Vapour CO_2
Intensity
1200
1250
1300
1350
1400
1450
1500
Raman Shift / cm^{-1}

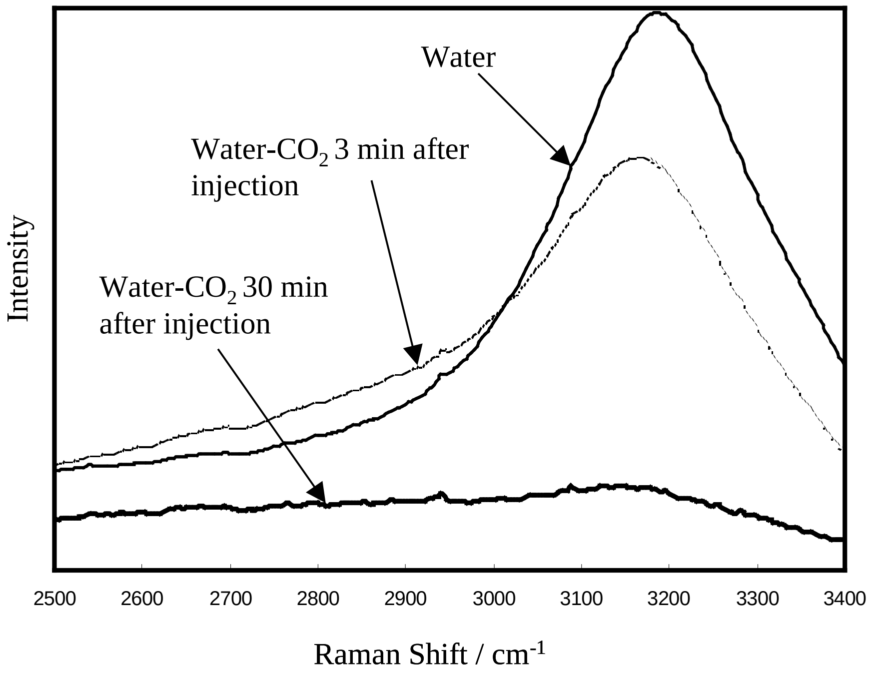
Water
Water-CO_2 3 min after injection
Water-CO_2 30 min after injection
Intensity
2500
2600
2700
2800
2900
3000
3100
3200
3300
3400
Raman Shift / cm^{-1}

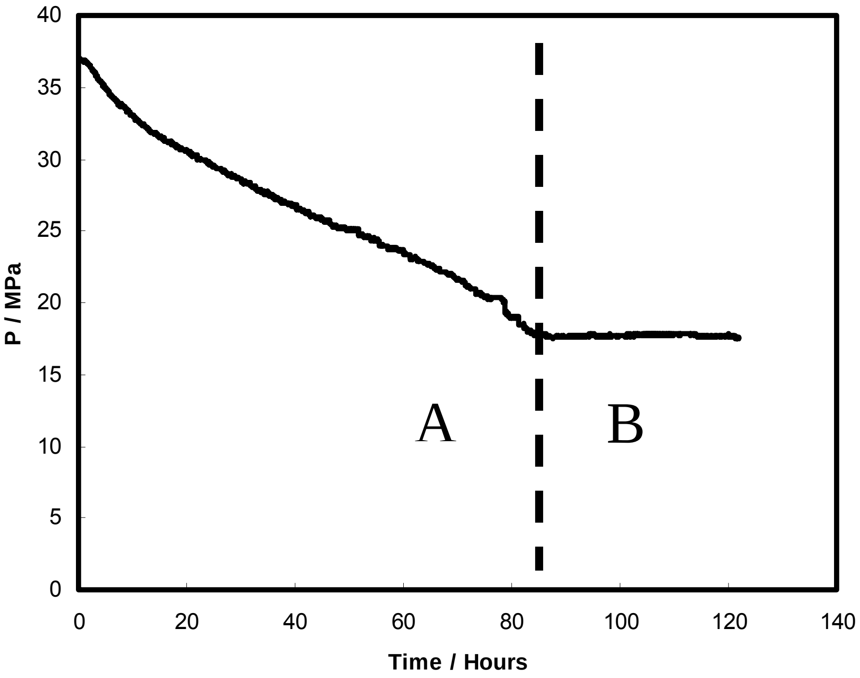

P / MPa
40
35
30
25
20
15
10
5
0
0
20
40
60
80
100
120
140
Time / Hours
A
B

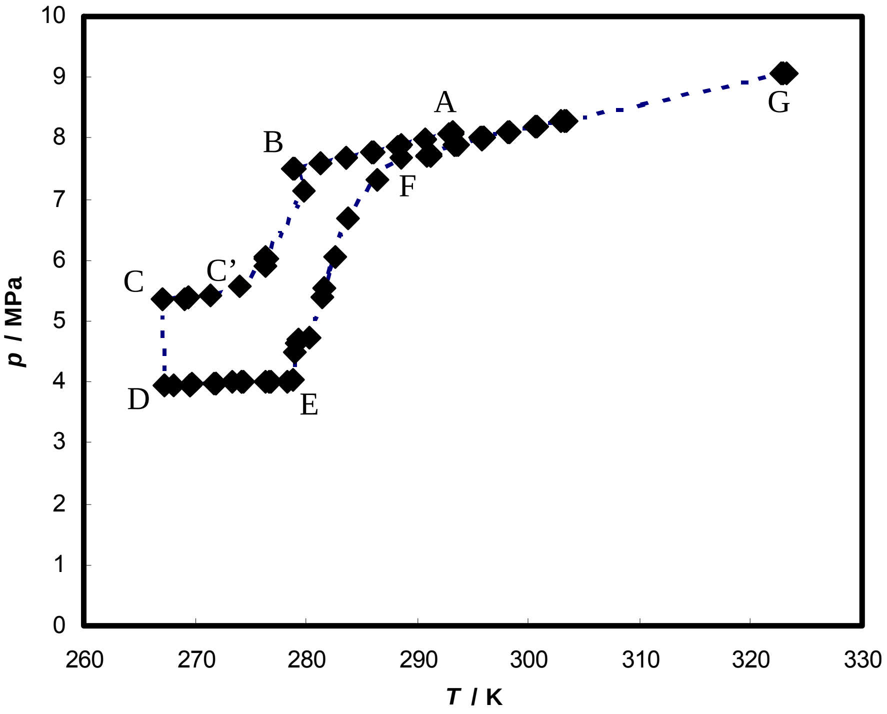
10
9
8
7
6
5
4
3
2
1
0
p / MPa
260
270
280
290
300
310
320
330
T / K
A
B
C
C’
D
E
F
G

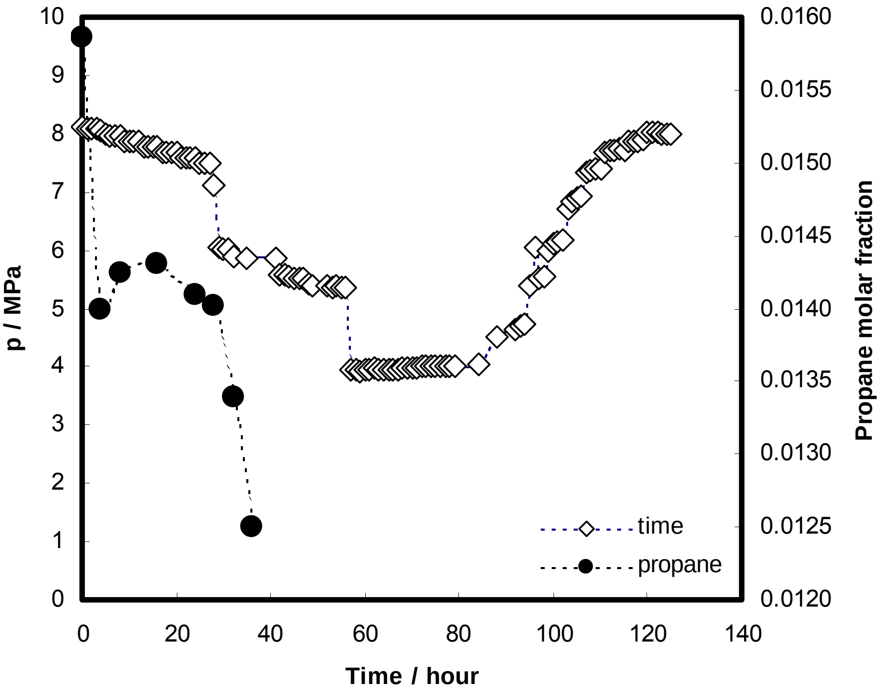

p / MPa
Propane molar fraction
Time / hour
0
1
2
3
4
5
6
7
8
9
10
0.0120
0.0125
0.0130
0.0135
0.0140
0.0145
0.0150
0.0155
0.0160
0
20
40
60
80
100
120
140
time
propane

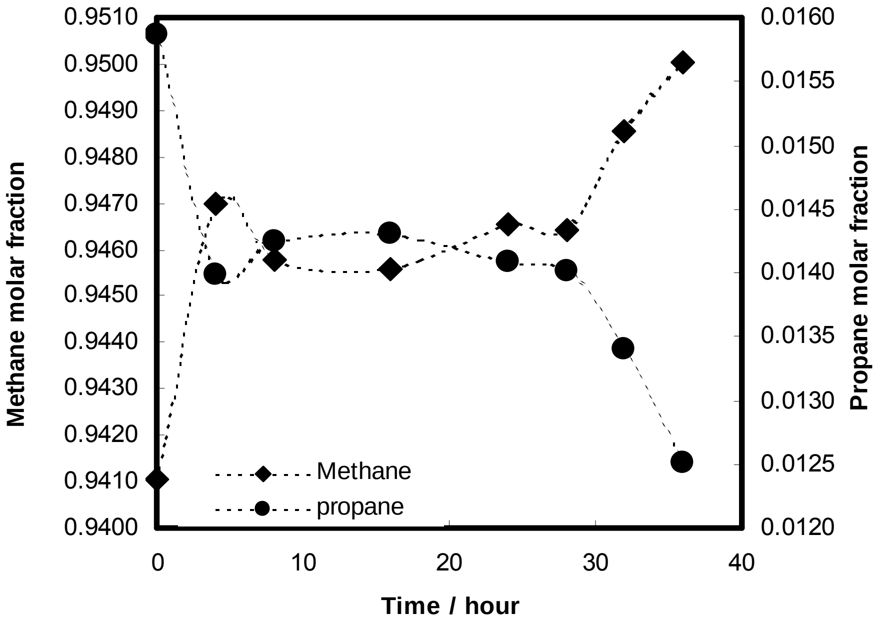
0.9510
0.9500
0.9490
0.9480
0.9470
0.9460
0.9450
0.9440
0.9430
0.9420
0.9410
0.9400
Methane molar fraction
0.0160
0.0155
0.0150
0.0145
0.0140
0.0135
0.0130
0.0125
0.0120
Propane molar fraction
0
10
20
30
40
Time / hour
Methane
propane

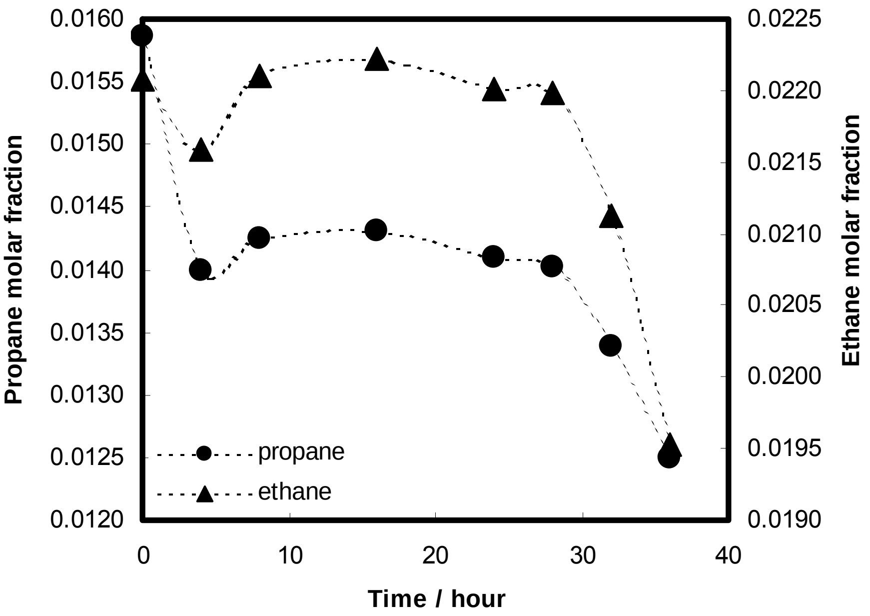
0.0160
0.0155
0.0150
0.0145
0.0140
0.0135
0.0130
0.0125
0.0120
Propane molar fraction
0.0225
0.0220
0.0215
0.0210
0.0205
0.0200
0.0195
0.0190
Ethane molar fraction
0
10
20
30
40
Time / hour
propane
ethane

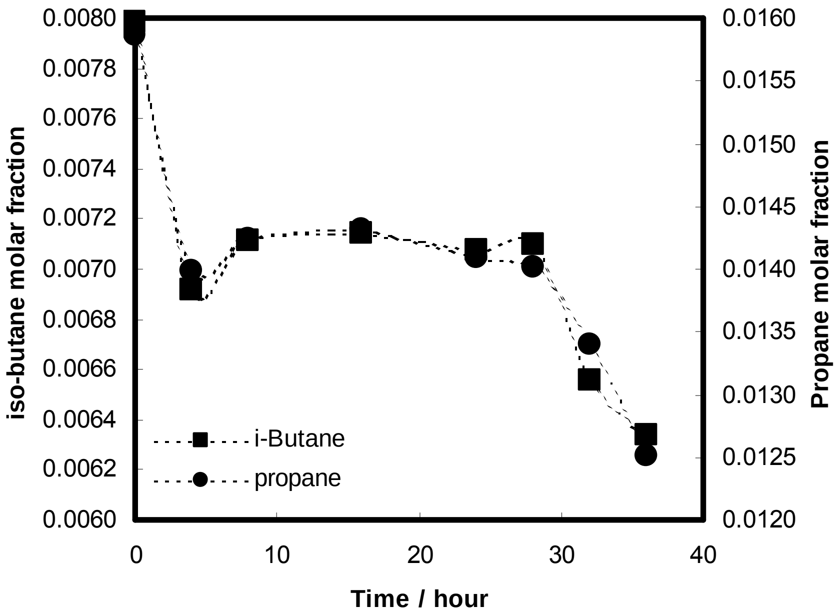
iso-butane molar fraction
0.0080
0.0078
0.0076
0.0074
0.0072
0.0070
0.0068
0.0066
0.0064
0.0062
0.0060
Propane molar fraction
0.0160
0.0155
0.0150
0.0145
0.0140
0.0135
0.0130
0.0125
0.0120
0
10
20
30
40
Time / hour
i-Butane
propane